

# Effect of varying film thickness on the properties of indium tin oxide films after temperature annealing

Forat H. Alsultany\*<sup>1</sup>, Naser M. Ahmed<sup>2</sup>, M. Z. Matjafri<sup>3</sup>

Nano-Optoelectronics Research and Technology Laboratory, School of Physics, University Science,  
11800 Penang, Malaysia

---

**Abstract:** Indium tin oxide thin films were deposited on glass substrates via high-temperature annealing technique and RF sputter coater system from a high density target (90 wt% In<sub>2</sub>O<sub>3</sub>–10 wt% SnO<sub>2</sub>). The effects of film thickness on the structural, electrical, and optical properties of the ITO films were investigated. The resulting ITO films with different thickness values were polycrystalline. The transmission, resistivity, and optical band gap of the ITO films decreased with increasing film thickness. By contrast, the grain size, intensity of the diffraction peak, and root-mean-square roughness increased with increasing film thickness. X-ray diffraction and field-emission scanning electron microscopy experiments were performed in this study.

**Keywords:** ITO thin film; RF sputtering; annealing; optical properties; structure; XRD; transmission; resistivity; sheet resistance; energy gap.

---

## Introduction

Transparent conductors have gained increasing interest since the first report of transparent conducting cadmium oxide films by Badeker (1907) [1]. Indium tin oxide (ITO) thin film are used as transparent conductive layers in various optoelectronic devices because of its high transparency to visible light and low electrical resistivity [2]. ITO is used as transparent conductors in liquid crystal display (LCD) [3], solar cells [4], and various light-sensitive solid-state devices. In organic light-emitting diodes (OLED) displays [5], ITO films with exceptionally smooth surface morphology are needed. High-quality ITO films have been prepared via various deposition methods, such as electron beam evaporation[6], thermal evaporation CVD [7], spray pyrolysis [8], pulse laser deposition [9], as well as DC and RF sputtering[10]. Post-deposition annealing at 350 °C in a furnace significantly improves the grain growth or crystallinity of ITO thin films, thereby resulting in reduced structural defects. This study focused on the effect of film thickness on the structural, electrical, and optical properties of ITO films.

## Experimental

The ITO thin films were deposited via RF sputtering onto a glass substrate by using an ITO target composite mixture (90 wt% In<sub>2</sub>O<sub>3</sub> and 10 wt% SnO<sub>2</sub>). The pressure before the deposition was approximately 10<sup>-7</sup> mbar. The highest power value delivered by the generator was 3000 W at 13.56 MHz radio frequency. The samples with thickness values of 50, 200, and 380 nm were prepared at 100 W. The glass substrates were cleaned via sonication with detergent (acetone and methanol), rinsed with deionized water for 15 min, blown dry with nitrogen gas, and finally dried in an oven at 120 °C for outgassing. Structural properties were identified via X-ray diffraction (XRD) and field-emission scanning electron microscopy (FESEM). XRD was employed at 2θ mode with Cu Kα radiation (XRD; Rigaku, D/MAX-Rc) at 1.54 Å. Resistivity values were measured using a Kethley 2400 source meter. Transmission curves were obtained using a spectrophotometer (Varian–Cary system 5000 UV-Vis-NIR spectrophotometer) to determine the optical transmission. Annealing was performed in air at 450 °C for 1 h.

## Results and discussions

For our results Fig. 1 shows the XRD patterns of the ITO thin films with different thickness values (50, 200, and 380 nm) annealed at 450 °C. Fig. 1(a) shows the XRD pattern of the 50 nm thick film, in which one major peak is found and one reflection from (222) plane with 30.566 intensity in the standard XRD data. Fig. 1(b) shows the XRD pattern for the 200 nm thick film, in which three major peaks are found and reflections from (211), (222), and (440) planes, with relative intensities of 21.48, 30.56, and 50.99, respectively. Fig. 1(c) shows the XRD pattern of the 380 nm thick film, in which five major peak are found with reflections from (211), (222), (400), (440), and (622) planes with

relative intensities of 21.48, 30.56, 30.43, 50.99, and 60.62, respectively, in the standard XRD data [11]. Reflected X-ray intensity depends on the penetration depth of X-ray [12]. For the 50 nm thick films, we obtained only the reflection at high intensity in the standard data, which is significantly small compared with those for thicker films. The absence of reflection from (211), (400), and (622) plains in the 50 nm thick film is not due to the orientation but to the sample thickness [11].

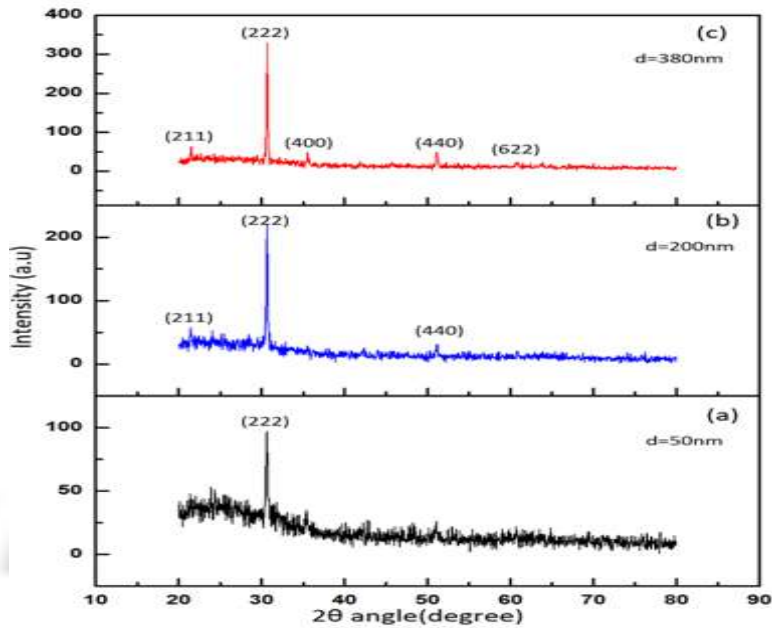


Fig. 1: XRD pattern of ITO films with different thickness.

The grain sizes were derived from the XRD spectra following the Scherer method [12]. Grain size  $D$  is given by  $D = K\lambda/\Delta(2\theta)\cos(\theta)$ , where  $\lambda$  is the X-ray wavelength ( $1.5406 \text{ \AA}$ ),  $K = (180/\pi) = 0.94$ , and  $\theta$  is the diffraction angle at which the peak of a particular orientation occurs. The grain size increased from 31.77 nm to 41.82 nm with increasing film thickness (Table 1).

Fig. 2 shows the FESEM images of the ITO thin films. The grain sizes increased with increasing film thickness.

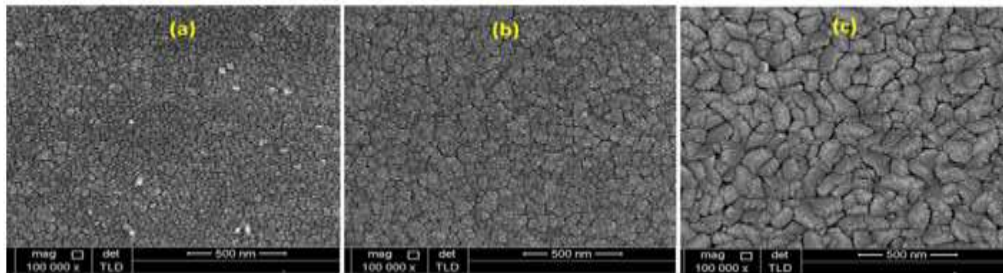


Fig. 2: FESEM of (a) 50 nm, (b) 200 nm, and (c) 380 nm thick ITO films.

Fig.3 shows the atomic force microscopic (AFM) surface images of a  $5 \mu\text{m} \times 5 \mu\text{m}$  ITO thin films. Fig. 3(a) observed shows that the 50 nm thick film has a smooth surface, good adherence to the substrate, and narrow size distribution. By contrast, the thicker films have hills and craters [Fig. 3(b,c)]. Thus, roughness increased with increasing film thickness. The root-mean-square (rms) roughness for the thin films increased from 1.7 nm at 50 nm thickness to 4.8 nm at 380 nm thickness (Table 1).

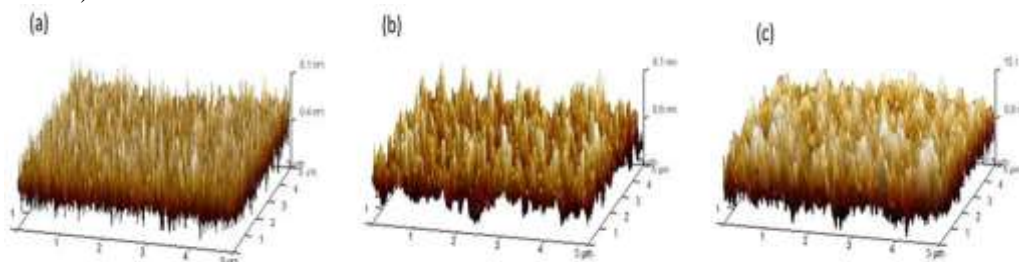


Fig. 3: Three-dimensional AFM images of the (a) 50 nm, (b) 200 nm, and (c) 380 nm thick ITO films.

Fig. 4 shows the variations in resistivity as a function of film thickness. The resistivity of the ITO films decreased with increasing film thickness, thereby suggesting that the electrical properties of the ITO films were strongly influenced by the film thickness. The lowest resistivity ( $3.8 \times 10^{-4} \Omega\text{-cm}$ ) was obtained from the 380 nm thick film (Table 1).

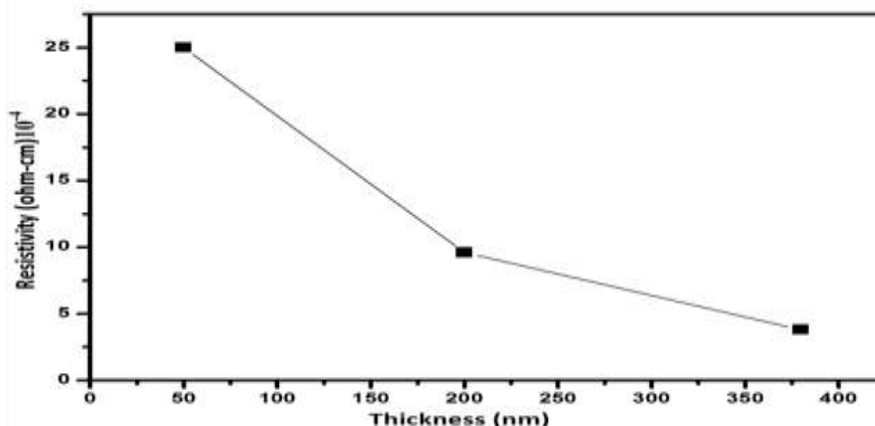


Fig. 4: Variations in resistivity of the ITO films.

Fig. 5 shows the optical transmission of the ITO films in the 300 nm to 800 nm wavelength range. The optical transmission of the ITO films decreased with increasing film thickness.

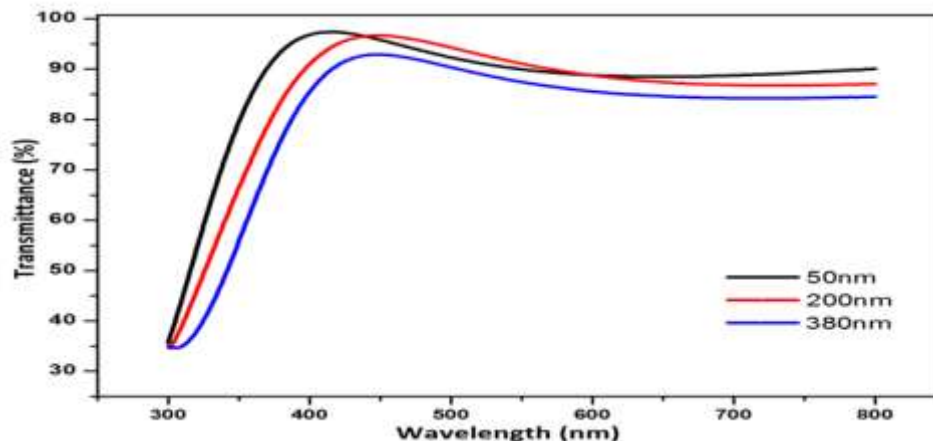


Fig. 5: Optical transmission spectra of the ITO thin films.

Fig. 6 shows the energy gaps of the ITO films. The energy gaps were calculated from the plot of  $(\alpha h\nu)^2$  versus  $h\nu$  for the ITO films. The absorption coefficients ( $\alpha$ ) were calculated from the optical transmission (T) by using the following equation:  $\alpha = (\ln 1/T)/D$ , where D is the film thickness. The photon energy ( $h\nu$ ) values were calculated using the following equation:  $h\nu = 1240/\lambda$ , where  $\lambda$  is the wavelength of the thin film [13]. The average energy gap decreased with increasing film thickness. The highest value of the energy gap (3.80 eV) was observed for the 50 nm thick film (Table 1).

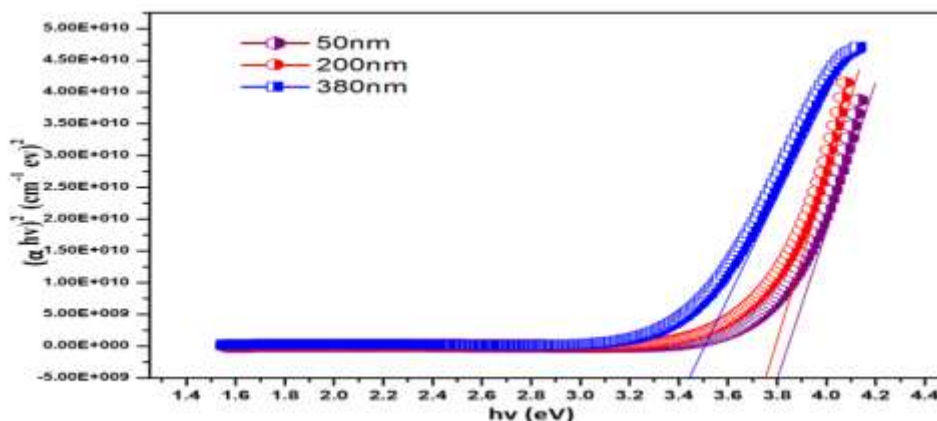


Fig. 6: Variations in the optical band gap of the ITO thin films

Tables 1: Grain size, roughness, and energy gap for the ITO thin films.

Film thickness (nm)	Grain size (nm)	rms roughness (nm)	Resistivity ( $\Omega$ -cm)	energy gap (eV)
50	31.77	1.71	$4.5 \times 10^{-3}$	3.80
100	34.32	2.54	$9.7 \times 10^{-4}$	3.75
380	41.82	4.81	$3.8 \times 10^{-4}$	3.44

### Conclusion

ITO thin films with different thickness values were deposited on glass via RF sputtering and high-temperature annealing (450 °C). The structural, optical, and electrical properties significantly depend on the film thickness. The transmittance, optical band gap, and resistivity decreased with increasing film thickness. By contrast, the rms roughness and grain size increased with increasing film thickness. These results showed that ITO films can be used as transparent electrode for OLED and touch screen monitors, as well as in piezoelectric crystal applications.

### Acknowledgement

We gratefully acknowledge the support of the school of physics University Science Malaysia under short term grant no 304/PFIZK/6312076.

### References

- [1]. Alex W. Hinrichsen "Baedeker's Travel Guides" 2nd edition. Published in electronic form by bdkr.com (2008).
- [2]. M. Baum, H. Kim, I. Alexeev, A. Piqué, M. Schmidt "Generation of transparent conductive electrodes by laser consolidation of LIFT printed ITO nanoparticle layers" *Applied Physics A* 111: (2013), 799-805.
- [3]. M. Sawada, M. Higuchi, S. Kondo, H. Saka "Characteristics of Indium-Tin-Oxide/Silver/Indium-Tin-Oxide Sandwich Films and Their Application to Simple-Matrix Liquid-Crystal Displays" *Japanese Journal of Applied Physics* 40 (2001) 3332.
- [4]. S.I. Na, S.S. Kim, J. Jo, D.Y. Kim "Efficient and Flexible ITO-Free Organic Solar Cells Using Highly Conductive Polymer Anodes" *Advances Materials* 20 (2008), 4061-4067.
- [5]. Y- L. Lee, K-M. Lee "Effect of Ambient Gases on the Characteristics of ITO Thin Films for OLEDs" *Transactions on Electrical and Electronic Materials* Vol. 10, No. 6, (2009).
- [6]. M. Yamaguchi, A. Ide-Ekessabi, H. Nomura, N. Yasui "Characteristics of indium tin oxide thin films prepared using electron beam evaporation" *Thin solid films* 447 (2004), 115-118.
- [7]. A. Amaral, P. Brogueira, C. Nunes de Carvalho, G. Lavareda "Early stage growth structure of indium tin oxide thin films deposited by reactive thermal evaporation" *Surface and Coatings Technology* 125 (2000), 151-156.
- [8]. S.M. Rozati, T. Ganj "Characterization of Transparent Conductive Thin Films of In<sub>2</sub>O<sub>3</sub>: Sn by Spray Pyrolysis Technique" *American Journal of Applied Science* 2 (2005), 1106-1108.
- [9]. J. Zheng, H.S. Kwok "Preparation of indium tin oxide films at room temperature by pulsed laser deposition" *Thin Solid Films* 232 (1993) 99-104.
- [10]. Daeil Kim "Effect of a TiO<sub>2</sub> Buffer Layer on the Properties of ITO Films Prepared by RF Magnetron Sputtering" *TRANSACTIONS ON ELECTRICAL AND ELECTRONIC MATERIALS* 14 (2013) 242-245.
- [11]. A. Pokaipisit, M. Horprathum, P. Limswan, "Influence of Annealing Temperature on the Properties of ITO Films Prepared by Electron Beam Evaporation and Ion-Assisted Deposition" *Kasetsart J. (Nat. Sci.)* 42(2008) 362 - 366.
- [12]. M Benoy, E. Mohammed, M. Suresh Binu, B. Pradeep "Thickness dependence of the properties of indium tin oxide (ITO) FILMS prepared by activated reactive evaporation" *Brazilian Journal of Physics* 39 (2009) 629-632.
- [13]. L. Kerkache, A. Layadi, F. Hadjersi, E. Dogheche, A. Gokarna, A. Stolz, M. Halbwax, J.P. Vilcot, D. Decoster, B. El Zein, S. S. Habib "Sputtered Indium Tin Oxide thin films deposited on glass substrate for photovoltaic application" Granada (Spain), 23th to 25th March, 2010.